Journal of Alloys and Compounds 509 (2011) 5761–5764

Contents lists available at ScienceDirect

Journal of Alloys and Compounds

journal homepage: www.elsevier.com/locate/jallcom

Martensitic transformation and magnetic properties in high-Mn content $Mn_{50}Ni_{50-x}In_x$ ferromagnetic shape memory alloys

H.C. Xuan, S.C. Ma, Q.Q. Cao*, D.H. Wang, Y.W. Du

National Laboratory of Solid State Microstructures and Key Laboratory of Nanomaterials for Jiang Su Province, Nanjing University, Nanjing 210093, People's Republic of China

ARTICLE INFO

Article history:
Received 25 November 2010
Received in revised form 4 January 2011
Accepted 7 January 2011
Available online 15 January 2011

Keywords:
Martensitic transformation
Magnetocaloric
Magnetoresistance

ABSTRACT

A series of $Mn_{50}Ni_{50-x}In_x$ (x = 9.75, 10, 10.25, 10.5 10.75, and 11) ferromagnetic shape memory alloys with Mn content as high as 50 at.% were prepared. The martensitic transformation (MT), magnetocaloric effect, and magnetoresistance in $Mn_{50}Ni_{50-x}In_x$ alloys were investigated. With x increasing from 9.75 to 11, the MT temperature decreased from 270 to 110 K and the Curie temperature of austenite remains relatively constant. Large positive magnetic entropy change and negative magnetoresistance were observed around MT temperatures in these alloys. Large magnetic entropy change and magnetoresistance would be ascribed to the temperature and magnetic field-induced MT in $Mn_{50}Ni_{50-x}In_x$ alloys.

1. Introduction

Heusler Ni–Mn–Ga alloys have drawn great attention in recent years since they show many functional properties around martensitic transformation (MT) [1–5]. Therefore, tuning MT in these alloys is of great importance and has been realized by adjusting the contents of Ni, Mn and Ga or doping other elements [4–6]. Up to now, many studies have focused on the off-stoichiometric Ni–Mn–Ga alloys in which the content of Ni is larger than that of Mn [4,5]. However, MT can also be observed in the system with high content of Mn even up to 50% (at.%), i.e. Mn_2NiGa [7]. It exhibits a MT around room temperature and distinguishes itself from the well-known Ni_2MnGa alloy by showing a much larger c/a ratio and much broader thermal hysteresis. An excellent two-way shape memory effect with strain of 1.7% and field controllable shape memory effect up to 4.0% have been observed in single crystalline Mn_2NiGa [7].

Recently, the new ferromagnetic shape memory alloys (FSMAs) Ni–Mn–X (X = In, Sn, Sb) have been extensively studied owing to their several interesting physical properties associated with MT [8–13]. It is well known that these alloys in some particular composition ranges undergo a first-order magnetic transition (FOPT) from a high symmetry phase (austenite) to a low symmetry phase (martensite) with decreasing temperature, associated with the sharp changes of magnetization, leading to large magnetoresistance (MR), giant magnetocaloric effects (MCE), and large magnetic-field-induced strain (MFIS) [10–16]. Similar to Ni_2MnGa, the Ni–Mn–X alloys with high Mn content, in which the content of Mn is larger than that of Ni, have rarely been investigated. According to our previous results, in the $Mn_{50}Ni_{40-x}Sn_{10+x}$ (x = 0, 0.5, and 1) alloys, the excess Mn atoms would occupy both Ni and Sn sites and result in a large exchange bias and different MT temperature [17]. In present study, we focused our study on Ni–Mn–In alloys and a series of MT were observed in the high-Mn content $Mn_{50}Ni_{50-x}In_x$ alloys. Moreover, large MCE and MR around MT temperature have been studied systemically.

2. Experiment

Polycrystalline ingots of $Mn_{50}Ni_{50-x}In_x$ (x = 9.75, 10, 10.25, 10.5, 10.75, and 11) alloys were prepared by arc-melting raw materials under a high-purity argon atmosphere. To attain a good compositional homogeneity, the samples were sealed in evacuated quartz tubes and annealed at 1073 K for 48 h, then quenched in cool water. The crystal structure was verified by X-ray diffraction (XRD) analysis using Cu Kα radiation at room temperature. The magnetization measurements were performed by a vibration sample magnetometer (7400 Lakeshore) under a magnetic field up to 12 kOe. The transport properties were measured in a physical property measurement system (PPMS, Quantum Design) using the four probe method.

3. Results and discussions

The XRD patterns of the $Mn_{50}Ni_{50-x}In_x$ (x = 9.75, 10, 10.25, 10.5, 10.75, and 11) alloys are shown in Fig. 1. All of them have a cubic $L2_1$ structure (austenite) at room temperature. Obviously, the diffraction peaks shift towards low angels with x increasing from 9.75 to 11, suggesting the increase in lattice constants. With the decrease of In content, a small extra phase appears [18], which indicated by asterisks in Fig. 1. Magnetization as a function of temperature for $Mn_{50}Ni_{50-x}In_x$ alloys was measured in a low magnetic

* Corresponding author. Tel.: +86 25 83594588; fax: +86 25 83595535.
E-mail address: qqcao@nju.edu.cn (Q.Q. Cao).

0925-8388/$ – see front matter © 2011 Elsevier B.V. All rights reserved.
doi:10.1016/j.jallcom.2011.01.073

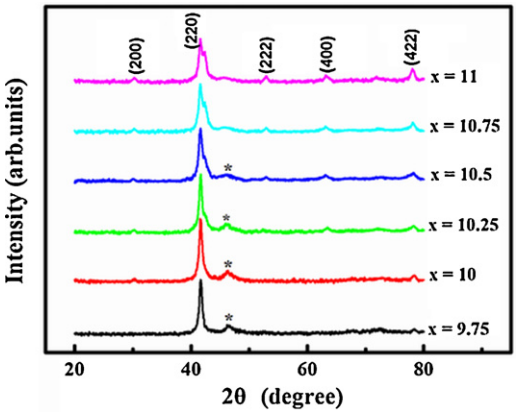

Fig. 1. Room temperature XRD patterns of $Mn_{50}Ni_{50-x}In_x$ (x = 9.75, 10, 10.25, 10.5, 10.75, and 11) alloys.

field of 100 Oe. Fig. 2(a) shows the M–T curves for $Mn_{50}Ni_{39.5}In_{10.5}$ alloy on heating and cooling. With decreasing temperature, a sharp increase of magnetization is observed at the ferromagnetic (FM) ordering temperature of the austenite of 340 K. Further decreasing temperature, a sudden drop of magnetization occurs at 190 K, which corresponds to the MT. Upon heating, the reverse MT from weak-magnetic martensite to FM austenite takes place at 188 K, while the FM transition of austenite occurs still at 340 K, suggesting the nature of FOPT for MT. Fig. 2(b) shows the M–T curves for all $Mn_{50}Ni_{50-x}In_x$ samples on heating under a magnetic field of 100 Oe. Obviously, a series of MT are observed in all alloys with high Mn content (50 at.%) in different temperature, which is associated with a sharp change of magnetization. Noted that most studies in Ni–Mn–In system have focused on tuning the ratio of Mn to In with a fixed Ni content of 50 at.% [11–13]. However, in present alloys, the MT temperatures can also be tuned in a wide range by fixing Mn content (50 at.%) with various Ni and In contents. From Fig. 2(b), the austenitic start temperatures (A_s) of $Mn_{50}Ni_{50-x}In_x$ alloys shift

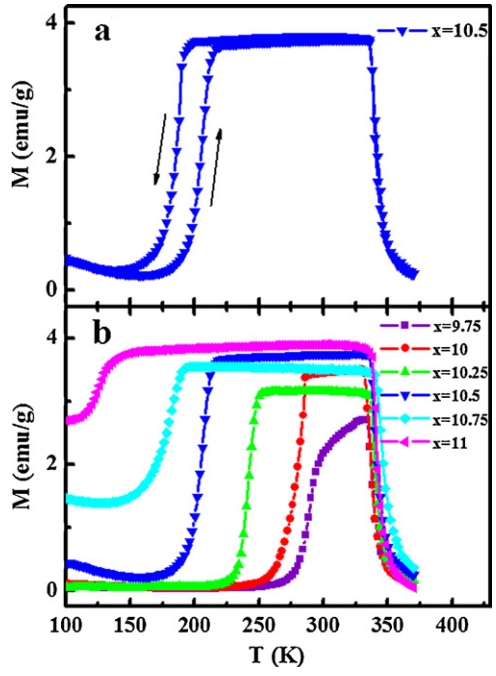

Fig. 2. Temperature dependence of magnetization under a magnetic field of 100 Oe for (a) $Mn_{50}Ni_{39.5}In_{10.5}$ alloy on heating and cooling and (b) $Mn_{50}Ni_{50-x}In_x$ (x = 9.75, 10, 10.25, 10.5, 10.75, and 11) alloys on heating.

Table 1
The values of austenitic start temperature (A_s), austenitic finish temperature (A_f), the Curie temperature of austenitic phase (T_C^A), valence electron concentration (e/a), refrigerant capacity (RC), and magnetic entropy change ΔS_M for $Mn_{50}Ni_{50-x}In_x$ (x = 9.75, 10, 10.25, 10.5, 10.75 and 11) alloys.

x	A_s (K)	A_f (K)	T_C^A (K)	ΔSM (J/kg K)	RC (J/kg)	e/a
9.75	270	300	337	2.3	27	7.8175
10	255	286	337	8.1	42	7.80
10.25	220	250	339	7.7	54	7.7825
10.5	188	215	340	7.2	61	7.765
10.75	150	189	342	5.6	45	7.7475
11	110	136	340	4.1	50	7.73

substantially towards lower temperature with increasing content of In, while the Curie temperature of the austenite phase remains almost unchanged. This behavior agrees in general with previously reports [11,12]. It is reported that characteristic temperatures in FSMAs are relative to the valence electron concentration e/a (electrons per atom) [17,19]. Here the valence electron is calculated as the number of 3d and 4s electrons of transition metals (Ni, Mn) and the number of 5s and 5p electrons of In. Since In has less valence electrons than Ni, increasing the content of In would result in an decrease of e/a, and consequently, MT temperature decreases from 270 to 112 K for x = 9.75 to 11 in $Mn_{50}Ni_{50-x}In_x$ alloys. The values of characteristic temperatures and e/a are listed in Table 1.

Isothermal magnetization curves M–H for $Mn_{50}Ni_{50-x}In_x$ (x = 9.75, 10, 10.25, 10.5, 10.75, and 11) alloys were measured around MT temperatures. Fig. 3 shows a series of M–H curves for $Mn_{50}Ni_{39.5}In_{10.5}$ alloy with a temperature interval of 1 K. It is obvious that the sample shows FM behavior above 210 K and weak magnetism below 200 K, which is consistent with the results of M–T. No obvious metamagnetic behavior can be observed between 200 and 210 K under the field of 12 kOe, suggesting that the applied magnetic field is not high enough to completely induce MT in $Mn_{50}Ni_{39.5}In_{10.5}$ alloy. It is well known that in the Mn rich $Ni_{50}Mn_{50-x}In_x$ alloys, the excess Mn atoms would occupy the In sites and the moments are coupled antiferromagnetically (AFM) to those of the surrounding Mn atoms on the regular Mn sites [9,17,19]. After the MT, the Mn–Mn distance would decrease due to the twinning of the martensitic phase, leading to the enhancement in the strength of the AF exchanges [9,17,19]. If the content of Mn is further increased to 50 at.% by decreasing Ni, i.e. $Mn_{50}Ni_{50-x}In_x$, the Mn atoms would occupy both the regular Ni and In sites, which would introduce more AFM regions [17].

The magnetic entropy changes (ΔS_M) were calculated from the isothermal magnetization curves using Maxwell relation [10,11,14]. ΔS_M as a function of temperature for $Mn_{50}Ni_{50-x}In_x$ (x = 9.75, 10, 10.25, 10.5, 10.75, and 11) alloys under the applied

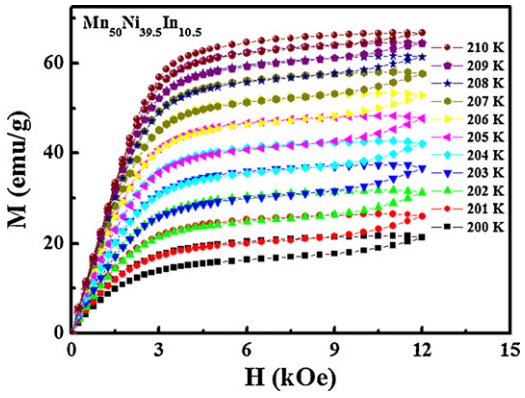

Fig. 3. Isothermal magnetization curves for $Mn_{50}Ni_{39.5}In_{10.5}$ alloy around MT temperature.

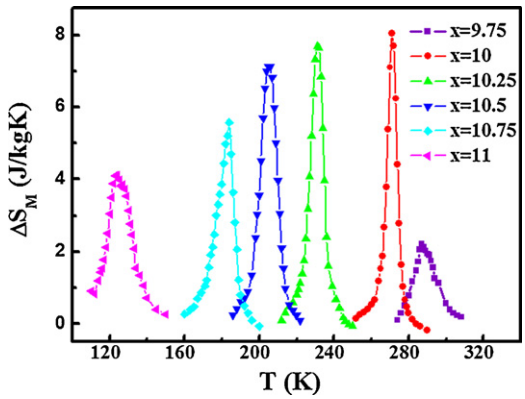

Fig. 4. Temperature dependence of ΔS_M in the magnetic field of 12 kOe for $Mn_{50}Ni_{50-x}In_x$ (x = 9.75, 10, 10.25, 10.5, 10.75, and 11) alloys.

field of 12 kOe is shown in Fig. 4. The maximum values of ΔS_M are 2.3, 8.1, 7.7, 7.2, 5.6, and 4.1 J/kg K for x = 9.75, 10, 10.25, 10.5, 10.75, and 11, respectively. These values are comparable to ΔS_M in $Gd_5Si_2Ge_2$ [20], Ni–Mn–Sn [10,14], and $Ni_{50}Mn_{50-x}In_x$ alloys [11], which display large MCE near the FOPT. The refrigerant capacity (RC) value, one useful parameter used to quantify the MCE properties, was calculated by integrating the $\Delta S_M(T, H)$ curves over the full width at half maximum [11]. The maximum value is 54 J/kg for x = 10.25, which is comparable with that in $Ni_{50}Mn_{34}In_{16}$ alloy under the same magnetic field [11]. The ΔS_M and RC values for different In contents are presented in Table 1. It can be seen that large low-field ΔS_M and RC can be obtained from 300 to 120 K by tuning the component of the Ni and In. Since MT temperatures of $Mn_{50}Ni_{50-x}In_x$ alloys can be easily tuned, it is possible to develop composites based on these alloys that exhibit large ΔS_M in a wide temperature range.

Nowadays, it is still controversial to calculate the value of ΔS_M by using Maxwell relation in the FOPT systems [21,22]. Some researchers think that there are some discrepancies between the MCE computed from specific heat measurements and magnetization measurements [21,22]. It is noticed that the entropy variations in $Ni_{45}Co_5Mn_{37.5}In_{12.5}$ single crystal determined using Maxwell and Clusius–Clapeyron relationships are comparable [23]. Moreover, the result roughly agrees with each other for ΔS_M of $Ni_{45}Co_5Mn_{36.5}In_{13.5}$ alloy calculated by Maxwell relation and that of $Ni_{45}Co_5Mn_{36.5}In_{13.5}$ alloy by DSC measurements [15,24]. Thus, the values of the ΔS_M can be calculated to some extent by Maxwell relation based on magnetization measurements in these Ni–Mn based FSMAs. Nevertheless, detailed experiments are still required for fully understanding the intrinsic MCE in these alloys.

Fig. 5(a) shows the temperature dependence of resistivity (ρ–T) for $Mn_{50}Ni_{39.25}In_{10.75}$ alloy on heating and cooling processes under zero-field. The resistivity of the alloy remains almost constant at low temperatures and drops abruptly around reverse MT temperature which corresponds to the phase transition between weak-magnetic martensite and FM austenite. Above reverse MT temperature, the resistivity increases slowly with increasing temperature, showing a typical metallic behavior. It is noted that the structure of martensite is different from that of austenite. So, the crystal symmetry changes through the MT, and the density of state in the vicinity of the Fermi level may be modified, which can lead to the sharp decrease of the electrical resistivity [13,25]. Upon cooling process, the similar behavior for resistivity can be observed. Obviously, the existence of a large thermal hysteresis between heating and cooling processes confirms the first order nature of MT.

The ρ–T curves for $Mn_{50}Ni_{50-x}In_x$ (x = 10.5, 10.75) alloys at 0 and 50 kOe on heating are plotted in Fig. 5(b). In the low and high temperature range, the value of resistivity at zero field is almost

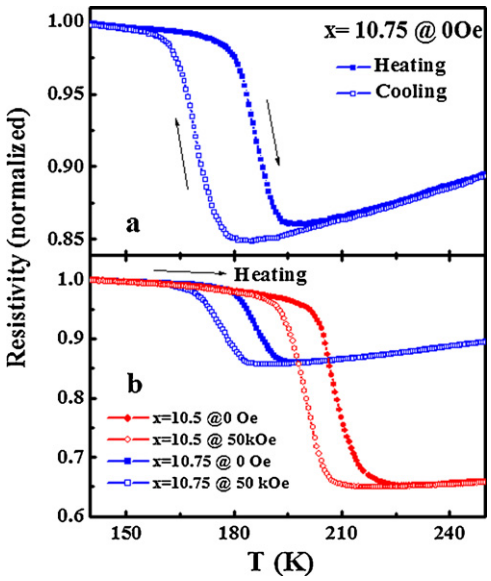

Fig. 5. Temperature dependence of resistivity for (a) $Mn_{50}Ni_{39.25}In_{10.75}$ alloy at zero field on heating and cooling and (b) $Mn_{50}Ni_{50-x}In_x$ (x = 10.5, 10.75) alloys at 0 and 50 kOe on heating.

the same with that at 50 kOe, suggesting that there is no obvious MR effect in martensite and austenite. It is well known that magnetic field can induce MT in Ni–Mn based FSMAs, and this phase transition is associated with drastic changes of electrical resistivity between martensite and austenite. Therefore, around MT temperature, the electrical resistance of these alloys can be effectively modified by a magnetic field. In addition, the reverse MT temperature decreased by 9 and 8 K under 50 kOe for the alloys with x = 10.75 and 10.5, respectively, indicating the effect of magnetic field on MT. Moreover, it is obvious that the changes of resistivity in the alloy of x = 10. 5 is larger than that of x = 10.75. As shown in Fig. 2(b), MT occurs between a FM austenite and a weak-magnetic martensite for x = 10. 5. But in the case of x = 10.75, since the Curie temperature of martensite is larger than MT temperature, a phase transition from FM martensite to FM austenite is observed with increasing temperature. It seems that the different magnetic state around MT would make a contribution to the different changes of resistivity in x = 10.75 and 10.5 alloys.

The variation of MR with temperature for $Mn_{50}Ni_{50-x}In_x$ (x = 10.5, 10.75) alloys is shown in Fig. 6. The MR is determined by using the relation $[\rho(H) - \rho(0)]/\rho(0)$. It is obvious that large MR is only observed around MT temperature. Under the field of

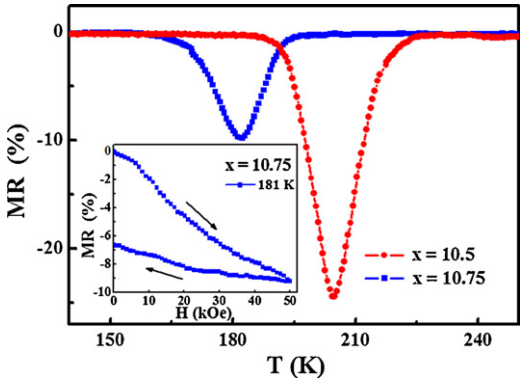

Fig. 6. Temperature dependence of MR for $Mn_{50}Ni_{50-x}In_x$ (x = 10.5, 10.75) alloys at a magnetic field of 50 kOe. Inset: Field dependence of MR for $Mn_{50}Ni_{39.25}In_{10.75}$ alloy at 181 K.

50 kOe, the negative peak values of MR are 10% and 24% for $x = 10.75$ and $x = 10.5$, respectively, which are slightly smaller than that in $Ni_{50}Mn_{50-x}In_x$ alloys [13]. As we know, martensite and austenite have different crystal structures, and consequently, different resistivities. Therefore, around the MT, with the variation of temperature and magnetic field, the electric structure together with the density of states near the Fermi surface should be modified, leading to the abrupt change of electrical resistivity and then resulting in a large MR. The inset presents the MR curves for $x = 10.75$ at 181 K. Before measurement, the sample was first cooled down to 100 K, far below the MT temperature, and then heated to the required temperature. The value of MR decreases gradually with increasing magnetic field, showing no obvious saturation even the field up to 50 kOe, since the applied field is still insufficient to fully induce MT. However, resistivity remains almost constant as the magnetic field decreases from 50 kOe to zero, implying that the return transition from austenite to martensite cannot be realized [26,27].

4. Conclusion

We have studied the phase transition, MCE and MR in high-Mn content $Mn_{50}Ni_{50-x}In_x$ alloys. MT can be observed in these high-Mn content alloys and tuned in a wide temperature range by adjusting the Ni and In contents. With x increasing from 9.75 to 11 on heating process, the reverse MT temperature decreases from 270 to 110 K and the Curie temperature of austenite remains relatively constant. Such behaviors are consistent with the dependence of transition temperature on the valence electron concentration e/a. Large MCE and MR effects, which are ascribed to the temperature and field induced MT, are observed around MT temperature. The $Mn_{50}Ni_{50-x}In_x$ alloys have large positive MCE, negative MR, adjustable MT temperature and low cost, which would be a multifunctional applied material candidate.

Acknowledgment

This work is supported by the National Basic Research Program of China (Grant No. 2005CB623605), National Natural Science Foundation of China (Grant No. 50701022 and 50831006), and NCET-08-0278.

References

[1] A. Sozinov, A.A. Likhachev, N. Lanska, K. Ullakko, Appl. Phys. Lett. 80 (2002) 1746–1748.
[2] S.J. Murray, M. Marioni, S.M. Allen, R.C. O'Handley, T.A. Lograsso, Appl. Phys. Lett. 77 (2000) 886–888.
[3] M.A. Marioni, R.C. O'Handley, S.M. Allen, Appl. Phys. Lett. 83 (2003) 3966–3968.
[4] C. Biswas, R. Rawat, S.R. Barman, Appl. Phys. Lett. 86 (2005) 202508.
[5] V.D. Buchelnikov, V.V. Sokolovskiy, H.C. Herper, H. Ebert, M.E. Gruner, S.V. Taskaev, V.V. Khovaylo, A. Hucht, A. Dannenberg, M. Ogura, H. Akai, M. Acet, P. Entel, Phys. Rev. B 81 (2010) 094411.
[6] T. Kanomata, Y. Kitsunai, K. Sano, Y. Furutani, H. Nishihara, R.Y. Umetsu, R. Kainuma, Y. Miura, M. Shirai, Phys. Rev. B 80 (2009) 214402.
[7] G.D. Liu, J.L. Chen, Z.H. Liu, X.F. Dai, G.H. Wu, Appl. Phys. Lett. 87 (2005) 262504.
[8] Y. Sutou, Y. Imano, N. Koeda, T. Omori, R. Kainuma, K. Ishida, K. Oikawa, Appl. Phys. Lett. 85 (2004) 4358–4360.
[9] P.J. Brown, A.P. Gandy, K. Ishida, R. Kainuma, T. Kanomata, K.U. Neumann, K. Oikawa, B. Ouladdiaf, K.R.A. Ziebeck, J. Phys.: Condens. Matter 18 (2006) 2249–2259.
[10] T. Krenke, E. Duman, M. Acet, E.F. Wassermann, X. Moya, L. Mañosa, A. Planes, Nat. Mater. 4 (2005) 450–454.
[11] A.K. Pathak, M. Khan, I. Dubenko, S. Stadler, N. Ali, Appl. Phys. Lett. 90 (2007) 262504.
[12] A.K. Pathak, B.R. Gautam, I. Dubenko, M. Khan, S. Stadler, N. Ali, J. Appl. Phys. 103 (07) (2008) F315.
[13] S.Y. Yu, Z.H. Liu, G.D. Liu, J.L. Chen, Z.X. Cao, G.H. Wu, B. Zhang, X.X. Zhang, Appl. Phys. Lett. 89 (2006) 162503.
[14] H.C. Xuan, D.H. Wang, C.L. Zhang, Z.D. Han, B.X. Gu, Y.W. Du, Appl. Phys. Lett. 92 (2008) 102503.
[15] R. Kainuma, Y. Imano, W. Ito, Y. Sutou, H. Morito, S. Okamoto, O. Kitakami, K. Oikawa, A. Fujita, T. Kanomata, K. Ishida, Nature 439 (2006) 957–960.
[16] J. Liu, S. Aksoy, N. Scheerbaum, M. Acet, O. Gutfltisch, Appl. Phys. Lett. 95 (2006) 232515.
[17] H.C. Xuan, Q.Q. Cao, C.L. Zhang, S.C. Ma, S.Y. Chen, D.H. Wang, Y.W. Du, Appl. Phys. Lett. 96 (2010) 202502.
[18] A.K. Pathak, I. Dubenko, S. Stadler, N. Ali, J. Phys. D: Appl. Phys. 41 (2008) 202004.
[19] T. Krenke, M. Acet, E.F. Wassermann, X. Moya, L. Mañosa, A. Planes, Phys. Rev. B 72 (2005) 014412.
[20] V.K. Pecharsky, K.A. Gschneidner, Phys. Rev. Lett. 78 (1997) 4494–4497.
[21] J.D. Zou, B.G. Shen, B. Gao, J. Shen, J.R. Sun, Adv. Mater. 21 (2009) 693–696.
[22] S. Das, J.S. Amaral, V.S. Amaral, J. Phys. D: Appl. Phys. 43 (2010) 152002.
[23] D. Bourgault, J. Tillier, P. Courtois, D. Maillard, X. Chaud, Appl. Phys. Lett. 96 (2010) 132501.
[24] L. Chen, F.X. Hu, J. Wang, J. Shen, J. Zhang, J.R. Sun, B.G. Shen, J.H. Yin, L.Q. Pan, J. Appl. Phys. 107 (09) (2010) A940.
[25] K. Koyama, H. Okada, K. Watanabe, T. Kanomata, R. Kainuma, W. Ito, K. Oikawa, K. Ishida, Appl. Phys. Lett. 89 (2006) 182510.
[26] H.C. Xuan, Y. Deng, D.H. Wang, C.L. Zhang, Z.D. Han, Y.W. Du, J. Phys. D: Appl. Phys. 41 (2008) 215002.
[27] V.K. Sharma, M.K. Chattopadhyay, K.H.B. Shaeb, S.B. Anil Chouhan, Roy, Appl. Phys. Lett. 89 (2006) 222509.